Discovery of a red and blue shifted iron disk line in the galactic jet source GRO J1655-40

M. Bałucińska-Church and M. J. Church

University of Birmingham, School of Physics and Astronomy, Birmingham, B15 2TT, UK e-mail: mjc@star.sr.bham.ac.uk, mbc@star.sr.bham.ac.uk

Accepted 17 December 1999. Received 24 August, 1999

ABSTRACT

We report the discovery of emission features in the X-ray spectrum of GRO J1655-40 obtained with RXTE during the observation of 1997, Feb 26. We have fitted the features firstly by two Gaussian lines which in four spectra analysed have average energies of 5.85 ± 0.08 keV and 7.32 ± 0.13 keV, strongly suggestive that these are the red and blue shifted wings of an iron disk line. These energies imply a velocity of ~ 0.33 c. The blue wing is less bright than in the calculated profiles of disk lines near a black hole subject to Doppler boosting, however known Fe absorption lines in GRO J1655-40 at energies between ~ 7 and 8 keV can reduce the apparent brightness of the blue wing. Secondly, we have fitted the spectra using the disk line model of Laor based on a full relativistic treatment plus an absorption line, and show that good fits are obtained. This gives a restframe energy of the disk line between 6.4 and 6.8 keV indicating that the line is iron K_{α} emission probably of significantly ionized material. The Laor model shows that the line originates in a region of the accretion disk extending from ~ 10 Schwarzschild radii from the black hole outwards. The line is direct evidence for the black hole nature of the compact object and is the first discovery of a highly red and blue shifted iron disk line in a Galactic source.

Key words: accretion, accretion disks – black hole physics – line: identification – binaries: close – stars: individual: GRO J1655-40 – X-rays: stars

1 INTRODUCTION

The X-ray nova GRO J1655-40 discovered with BATSE (Zhang et al. 1994) is one of the two only definite Galactic superluminal jet sources: GRO J1655-40 and GRS 1915+105 (Mirabel & Rodriguez 1994). These two sources are also transient whereas the source SS 433 with velocity in the jets of 0.26 c is persistent. Radio images of the source showed condensations moving in opposite directions (Tingay et al. 1995). The apparent superluminal motion implies that the emitting plasma has velocity close to c, in fact 0.92 c (Hjellming & Rupen 1995). Initially, X-ray outbursts were separated by \sim 120 d (Zhang et al. 1995), and on 1996, April 25 an outburst began lasting 16 months as shown by the RXTE ASM (Sobczak et al. 1999). By the time of this outburst, the strong radio activity had ceased, although radio emission was detected again on 1996, May 29 (Hunsted & Campbell-Wilson 1996). Lack of radio detection after that date despite regular monitoring (Tingay 1999) implies that the jets had ceased to exist.

The optical observation of 1996, March provided a mass of the central objects of $7.02\pm0.22~M_{\odot}$ and an inclination

angle of $69.5\pm0.08^{\circ}$ (Orosz & Bailyn 1997). An inclination of $67.2\pm3.5^{\circ}$ was found by van der Hooft et al. (1998). GRO J1655-40 is thus generally accepted to be a Black Hole Binary, the only Galactic jet source with mass determination evidence for its black hole nature.

Several observations were made with ASCA, the first on 1994, August 23 and on 1997, Feb 26–28 an observation lasting one orbital cycle was made during which the RXTE observation discussed here was also made. Iron absorption line features were found at ~ 6.6 keV and ~ 7.7 keV when the source was less bright (0.27–0.57 crab), and at \sim 7 keV and $\sim 8 \text{ keV}$ when the source was brighter (2.2 crab), and these were identified with K_{α} and K_{β} lines of Helium-like and Hydrogen-like iron respectively. In the observation of 1997, Feb 26–28, a broad absorption feature at $\sim 6.8 \text{ keV}$ was seen, thought to be a blend of He-like and H-like lines (Yamaoka et al. 1999). Sobczak et al. (1999) found evidence for an iron edge at 8 keV. X-ray dipping has been observed in GRO J1655-40 and many short and deep dips similar to the those in Cygnus X-1 (Bałucińska-Church et al. 1999) are seen.

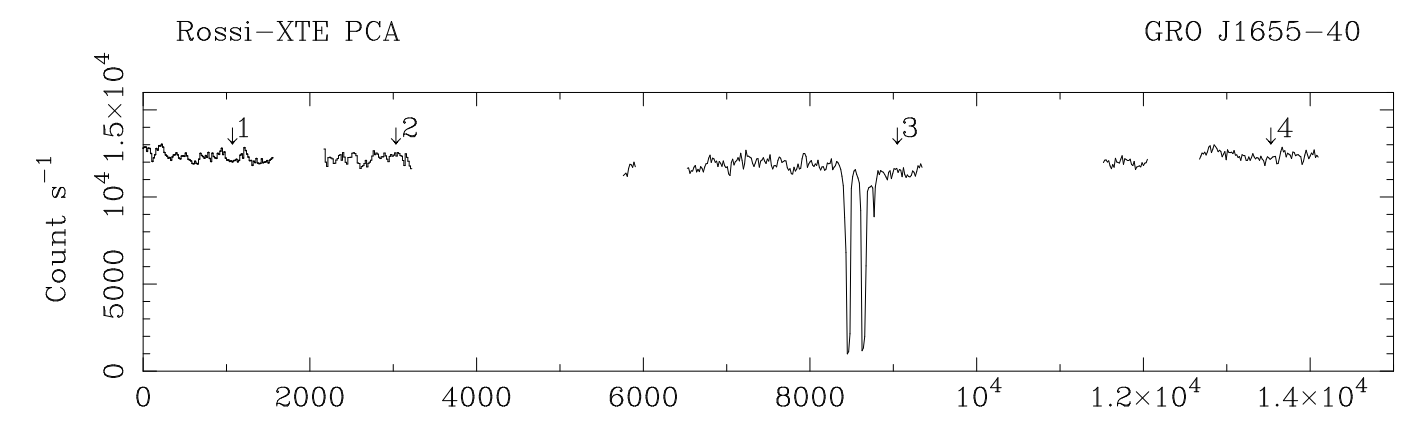


Figure 1. PCA light curve in the energy band 2 – 30 keV with 16 s binning after deadtime correction

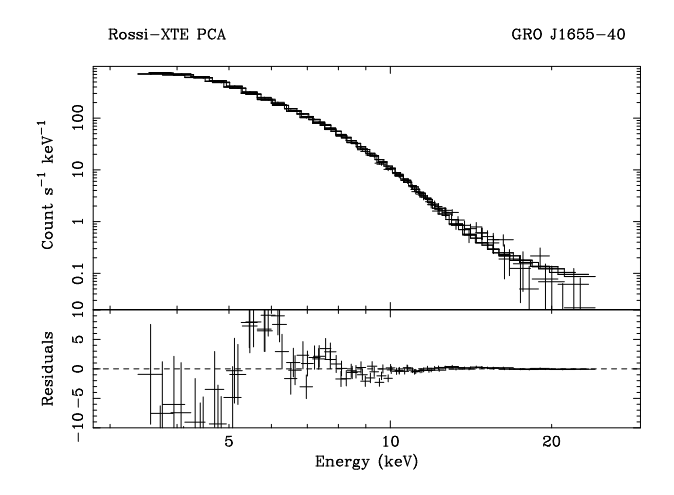


Figure 2. Spectrum of a single dataset with residuals; data from PCUs 0, 1 and 4 are shown which were fitted simultaneously

2 ANALYSIS AND RESULTS

The observation of GRO J1655-40 analysed here took place on 1997, Feb 26 lasting 14,600 s and had an exposure of 7.6 ks. Data from the PCA instruments in "Standard 2" mode are presented. Data were screened by selecting for angular distance less than 0.02° . The PCA consists of 5 Proportional Counting Units (PCU0 - 4); spectra were extracted for each PCU separately but only units 0, 1 and 4 were used because of the consistently higher values of χ^2 found in fitting data on the Crab Nebula with PCUs 2 and 3 (Sobczak et al. 1999). Figure 1 shows the light curve from all 5 PCUs of the PCA with a binning of 16 s. Strong dipping is seen at 8.5 ks. Four spectra were selected at different times during the observation avoiding the dips; these are indicated by arrows in Fig. 1, and are labelled spectrum 1 to spectrum 4. The third of these (at ~ 9 ks) follows a dip, and may have slightly reduced intensity. Results from 3 further spectra not presented gave similar results.

Spectra were accumulated over times averaging 140 s, equivalent to ${\sim}340{,}000$ counts per spectrum. Data were used between 3.5 - 25 keV. Primitive channels were regrouped in 2s between channels 30 and 39 (13 –16 keV) and in 4s above channel 40, and systematic errors of 1% added. Back-

ground subtraction was carried out using standard background models and instrument responses from 1998, Nov 28 used. Spectra from each time interval were extracted for PCUs 0, 1 and 4 and these were fitted simultaneously with a variable normalization allowed between the PCUs in the fitting. A number of spectral models were investigated. Simple one-component models were not able to fit the spectra and a good fit to the continuum was obtained with a two-component model consisting of a disk blackbody plus a power law component. The luminosity $(0.1-100~{\rm keV})$ was $9.7\times10^{37}~{\rm erg~s}^{-1}$ with the disk blackbody constituting 89% of the total and the power law 11%.

However, for the continuum-only model, the χ^2 per degree of freedom (dof) was poor, typically 130/91 and positive residuals could be seen in the spectra as shown in the example of Fig. 2 (spectrum 3); and these data are re-plotted in the form of ratios of the data to the best-fit model for each of the 4 datasets in Fig. 3. Strong line features at ~ 5.8 keV and ~ 7.3 keV can be seen in all of the spectra. Note that in the ratio plots, the lower energy part of the line is reduced compared with the higher energy part because of the decreasing continuum, so that the line centre appears to be at higher energy than its true value shown in the residual plots. The 4 spectra were re-fitted with 2 Gaussian lines added to the model. There was a marked improvement in the quality of fit, with an average value of χ^2/dof of 70/85. Results for all 4 spectra are shown in Table 1, where values of χ^2 are compared with values for the continuum model alone. F-tests showed that the addition of 2 lines was significant at >>99.9% confidence. Fig. 4 shows the spectrum of Fig. 2 with 2 lines added to the model. Equivalent widths (EW) were derived for each Gaussian component, treating the red and blue wings as separate lines and the red wing had a mean EW of 70 eV and the blue wing a mean EW of 160 eV.

Absorption features can also be seen in the spectra, for example, at $\sim 8.9~\rm keV$ in spectrum 1 (lowest panel). This feature can be seen in all 4 spectra, and there is some evidence for small changes in its energy. Spectrum 3 also apparently has an absorption line or edge at $8.2~\rm keV$, and this may be indicative that the data are not completely out of the dip. To investigate this point further, dip spectra were examined in relatively shallow dipping in which the spectrum is not modified in a major way by absorption. A spectrum was se-

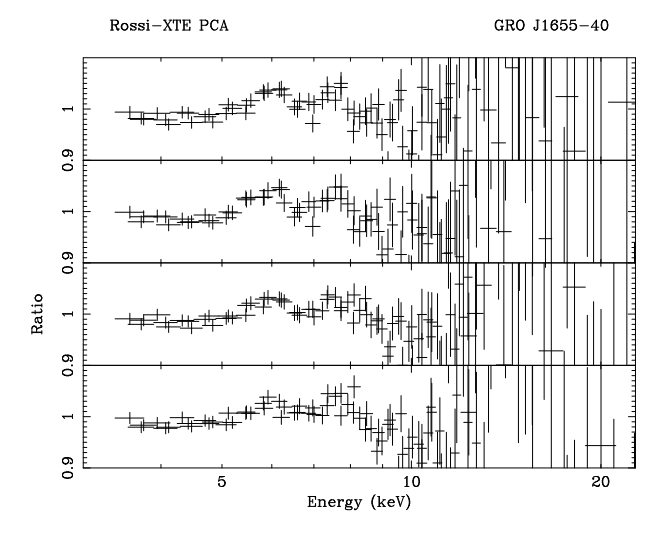


Figure 3. Ratios of the data to the models for the 4 spectra indicated in Fig. 1. The lowest panel shows spectrum 1

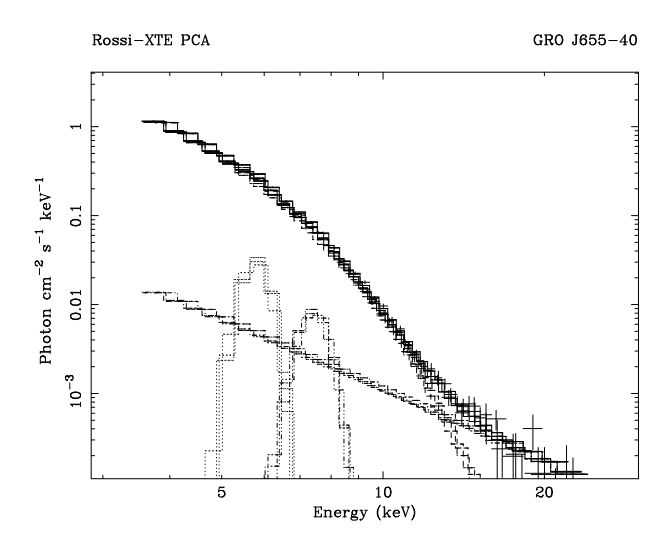


Figure 4. Unfolded spectrum of the best-fit to spectrum 3 including 2 Gaussian lines

lected in the intensity band 6100-6900 count s⁻¹ from Fig. 1 and the continuum fitted with an appropriate model with partial covering of the disk blackbody plus power law. In this case, the ratio plot showed an even stronger depression at \sim 8 keV than that of spectrum 3 in Fig. 3,

Although we have detected clear absorption features in the spectra, we can also ask whether the spectra may be modelled by addition of a postulated, but undetected, absorption feature at an energy between the red and blue emission peaks; i.e. by modelling the valley between the emission peaks without requiring there to be emission. The continuum-only model leaves positive residuals at ~ 5.8 and ~ 7.3 keV as can be seen in Fig. 2 and Fig. 3. Since the continuum is well-fitted (as shown by the χ^2 /dof for the best-fit models), these positive residuals are in no way model dependent, and so are strong evidence for the disk line. Thus it is impossible for the positive residuals to be removed by adding

Table 1. Line parameters from best fit spectral fitting results for spectra 1-4 using a model consisting of a disk blackbody + power law + 2 Gaussian lines. χ^2 values are also shown for the best continuum fits without emission lines (RH column)

| | E_1 (keV) | E_2 (keV) | $\frac{\mathrm{EW}_{1}}{\mathrm{(eV)}}$ | $\frac{\mathrm{EW}_2}{\mathrm{(eV)}}$ | χ^2/dof | χ^2/dof |
|------------------|--|--|---|---------------------------------------|----------------------------------|--------------------------------------|
| 1 2 3 4 | $5.82_{-0.17}^{+0.10} \\ 5.79_{-0.30}^{+0.09} \\ 5.79_{-0.21}^{+0.15} \\ 5.98_{-0.19}^{+0.11}$ | $7.20_{-0.59}^{+0.22} \\ 7.17_{-1.93}^{+0.43} \\ 7.43_{-0.58}^{+0.20} \\ 7.47_{-0.22}^{+0.13}$ | 51 66 99 62 | 210 209 135 81 | 79/85 60/85 59/85 80/85 | 153/91 123/91 119/91 135/91 |

an absorption line. It is confirmed by spectral fitting tests that the positive residuals cannot be removed in this way.

Fitting the spectra with two emission lines was the obvious way of investigating the energies of the emission features. The fact that the feature energies are consistent with red and blue shifted iron disk line emission is strong evidence that the features are iron disk line emission (the radio jets having ceased to exist) and makes it unlikely that these features are coincidentally at these energies and have another origin. The intensity of the blue wing of a disk line is however, expected to be higher than that of the red wing (Fabian et al. 1989; Laor 1991), whereas we find the blue wing intensity to be generally rather less than that of the red wing. The absorption features detected in ASCA and in the present work at energies above 6.6 keV can modify the observed broad disk line considerably, and we require absorption at about the energy of the blue wing for our results to be consistent with a disk line. Consequently, we have carried out fitting with a model containg the Laor disk line model in 'Xspec' added to the disk blackbody plus power law continuum components, plus an absorption line. Stable, free fitting results were obtained for all four spectra with this model and results are shown in Table 2. Values of the restframe energy varied between 6.4 keV and 6.8 keV with a mean of 6.56 keV. The energy of the absorption line was well-constrained since a large residual at a well-defined energy would result from the blue wing of the Laor model if the absorption line was omitted. Line energies varied between 7.0 and 7.3 keV. χ^2/dof values were similar to those obtained with two emission lines, varying between 60/84 and 87/84. The inner radius of the disk line emission region r₁ was found to be $\sim 10r_S$; r_2 was $\gtrsim 50r_S$, but was poorly constrained. We have thus shown that it is possible to fit the spectra with a model based on the assumption that the blue disk line wing appears relatively weak because of absorption at \sim 7 keV. It can be argued that the Laor model is preferred because it contains the correct line shape and two emission lines do not. On the other hand, the two emission line model is better able to determine red and blue energies as there is no complicating extra absorption component in the model. However, the line energies must be interpreted as an average over the inner disk. Finally, we note that we do not require absorption at exactly the energies derived above to reduce the observed flux of the blue wing; we are not attempting to fit all of the absorption features in the spectrum and various absorption features at 7 - 8 keV would be capable of reducing the blue wing flux.

Finally, we have tested whether a reflection component can be detected in GRO 1655-40, i.e. a component spectrally

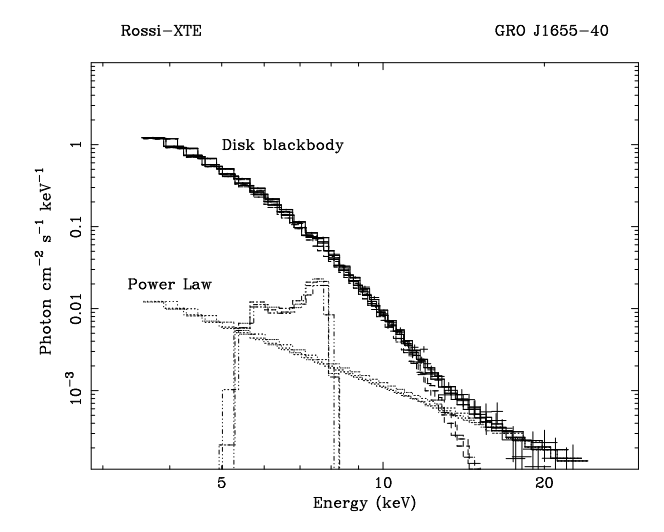


Figure 5. Best fit Laor disk line + absorption line model for spectrum 1. The disk blackbody, power law and Laor components are shown. The absorption line can not be plotted as it has negative normalization. The strong dominance of the blackbody emission can be seen.

different from the incident power law (see Ross, Fabian & Young 1999). To do this, we added the 'pexriv' component in Xspec to our best-fit models (Magdziarz & Zdziarski 1995), although this model may be inaccurate for high values of ξ (Ross et al. 1999). This was done for the two emission line models and for the Laor disk line plus absorption line models. Our results for the disk line energies and for the absorption line indicate an ionized medium and so we have allowed the ionization parameter ξ in the reflection model to vary between 500 and 10⁴. The reflection component normalization and power law index were chained to the values of the power law. We note however, that without the reflection component, for both the two emission line and Laor model fitting, χ^2/dof was already acceptable. Fitting with a reflection component added showed that there was no reduction in χ^2 . the upper limit flux of the pexriv reflection component was 1% of the total flux at 7 keV. For $\xi < 10^4$, the actual contribution of a reflection component would be less than 1%. We thus conclude that we have not detected a reflection component. If a reflection component exists at a flux level of $\lesssim 1\%$, it would not be possible for the edge in this component to modify in any significant way the values we have derived for red and blue wing energies, widths and EWs. In this source the blackbody strongly dominates the spectrum with 90% of the luminosity, see Fig. 5 above, unlike in Cygnus X-1 in the Low State (e.g. Bałucińska-Church et al. 1995) where the power law strongly dominates. The reflection component in pexriv is a fraction of the underlying power law of the order of 10%, and thus we expect the contribution of a reflection component to be small.

3 DISCUSSION

We have presented evidence for a broad emission feature in the X-ray spectrum of GRO J1655-40 having red and blue wings which we have modelled by two Gaussian lines and also using the Laor model plus an absorption line. Using

Table 2. Best fit spectral fitting results for spectra 1-4 using a model consisting of a disk blackbody + power law + Laor disk line model + absorption line.

| | $\frac{E_{rest}}{(keV)}$ | ${ m r_1} \ ({ m r_S})$ | $egin{array}{c} m r_2 \ (m r_S) \end{array}$ | E_{abs} (keV) | $\chi^2/{ m dof}$ |
|------------------|---|---|--|---|----------------------------------|
| 1 2 3 4 | $\begin{array}{c} 6.79_{-0.33}^{+0.13} \\ 6.54_{-0.16}^{+0.08} \\ 6.43_{-0.05}^{+0.06} \\ 6.47_{-0.16}^{+0.21} \end{array}$ | $10_{-6}^{+24} \\ 13_{-12}^{+10} \\ 9_{-9}^{+33} \\ 9_{-4}^{+12}$ | $41^{+115}_{-14} \\ 56^{+140}_{-24} \\ 75^{+125}_{-45} \\ 40^{+160}_{-15}$ | $7.30_{-0.67}^{+0.31}$ $7.10_{-0.19}^{+0.15}$ $6.99_{-0.21}^{+0.06}$ $6.96_{-0.17}^{+0.06}$ | 87/84 75/84 60/84 80/84 |

the first model, the line components have high significance as shown by F-tests, and the average line energies obtained fitting two emission lines from all 4 datasets analysed are $5.85\pm0.08~\rm keV$ and $7.32\pm0.13~\rm keV$. Given the inability to fit the spectra without emission lines, and given these line energies, it is likely that the emission is iron emission. From the fact that radio emission was switched off before the observation discussed, the lines almost certainly originate in the disk.

We have also fitted the spectra with a model consisting of continuum components plus a Laor disk line plus an absorption line, and conclude that the blue wing intensity less than expected can be explained by absorption at \sim 7 keV reducing the observed flux of the blue wing. This can be either iron K_{α} or K_{β} absorption. The results for this model give somewhat smaller restframe energies than derived from the two emission line model, the mean value being 6.56 ± 0.14 keV compared with $6.88\pm$ keV.

Firstly, we will compare our results with those obtained using ASCA. In the observations of 1994 - 1996, the energies at which iron absorption lines were detected were $\sim 6.6 \text{ keV}$ and ~ 7.7 keV for the source at lower intensity, and ~ 7 keV and ~ 8 keV when brighter (Ueda et al 1998). In the RXTE data however, we see evidence for an absorption feature at \sim 9 keV and for an absorption feature at 8 keV in spectrum 3. In the ASCA observation made on 1997, Feb 26–28 which included the RXTE observation, the total spectrum containing all data showed broad absorption at 6.7 keV thought to be a blend of He-like and H-like iron K_{α} lines (Yamaoka et al. 1999). This energy corresponds approximately to the position of the neck between the red and blue peaks that we detect. The ASCA spectra do show some evidence for emission however (i.e positive residuals), particularly when the source is not very bright (Fig. 3 of Ueda et al. 1998). It is not clear at this stage why emission features were not seen more clearly in ASCA; one possibility is that the emission may vary with time, and the ASCA spectra were integrated over relatively long periods leading to smearing of the emission.

Using our results from fitting two emission lines, the relativistic Doppler formula can be used with the mean energies of the red and blue wings $E_1=5.85$ keV and $E_2=7.32$ keV to solve for the velocity $\beta=v/c$ and the restframe energy of the disk line. This gives a mean restframe energy of 6.88 ± 0.12 keV and a mean $\beta=0.33\pm0.02$ for an inclination angle of 70° . The mean of E_1 and E_2 has an average of 6.58 ± 0.10 keV over the four spectra so that the redshift is 0.3 keV, i.e. z=0.046. This is partly gravitational redshift and partly the transverse Doppler effect. A gravitational redshift of 0.046 would be produced by emission at $\sim 12r_S$.

Results from the Laor model give a mean restframe energy of 6.56 ± 0.14 keV. We conclude that the restframe energy is between 6.4 and 7.0 keV indicating Fe K_{α} emission. The exact ionization state is not clear; the mean of $6.56~\mathrm{keV}$ implies Fe XXII. The Laor model fitting further provided the inner and outer radii of the disk line emission region r₁ $\sim 10 r_S$ and $r_2 \gtrsim 50 r_S$. It may be thought that emission from different radii would tend to smear out the wings; however, simulations show that this does not take place for emission between $10 - 100 r_S$, or even for emission between $10 - 200 r_S$. The inner radius of the emission region is more important, and if we allow emission from $1-10r_S$, there is smearing out because of the strong emission from inner radii and changing energy shifts. However, it is likely that the disk inside $10r_S$ is totally ionized by X-ray emission so that no lines are produced and large-scale smearing out does not occur.

The ASCA observation of 1997, February spanning one orbital cycle, detected an absorption line at $\sim\!6.8$ keV at all orbital phases, showing that the absorbing material was not confined to part of the accretion disk structure (Yamaoka et al. 1999) as in LMXB. Moreover, the line energies seen generally in ASCA were H-like or He-like showing that the absorbing plasma was highly ionized. Our observation of highly broadened iron emission clearly shows the line to originate in the inner, highly ionized, disk. The location of the absorber is however, not so clear.

Further observation and detailed analysis is clearly needed to explain the observed spectral features which are complex, the absorption features in particular, appearing to change with source intensity. GRO J1655-40 offers probably the best opportunity of studying disk lines strongly affected by gravitational and Doppler effects because of the high inclination at which it is seen. Our detection of the red and blue shifted wings at energies of 5.8 and 7.3 keV is direct evidence for the black hole, since a splitting as wide as this cannot be produced by a neutron star and is the first detection of a red and blue shifted disk line in a Galactic source.

4 ACKNOWLEDGMENTS

We would like to thank Prof. Hajime Inoue for valuable discussions on the relation between the emission features reported here and absorption features discovered with ASCA.

REFERENCES

Bałucińska-Church M., Church M. J., Charles P. A., Nagase F., LaSala J., Barnard R., 1999, MNRAS *In Press*

Bałucińska-Church M., Belloni T., Church M. J., Hasinger G., A&A 302, L5

Fabian A. C., Rees M., Stella L., White N. E., 1989, MNRAS, 238, 729

Hjellming R. M., Rupen M. P., 1995, Nature, 375, 464

Hunstead R. W., Campbell-Wilson D., 1996, IAU Circ. 6410

Laor A., 1991, ApJ, 376, 90

Magdziarz P., Zdziarski A. A., 1995, MNRAS, 273, 837

Mirabel I. F., Rodriguez L. F., 1994, Nature, 371, 46

Orosz J. A., Bailyn C. D., 1997, ApJ, 477, 876

Ross R. R., Fabian A. C., Young A. J., 1999, MNRAS 306, 461

Sobczak G. J., McClintock J. E., Remillard R. A., Bailyn C. D.,

Orosz J. A., 1999, ApJ, 520, 776

Thorne K. S., 1974, ApJ, 191, 507

Tingay S. J., et al. 1995, Nature, 374, 141

Tingay S. K., 1999 Priv. Comm.

Ueda Y., Inoue H., Tanaka K., Ebisawa K., Nagase F., Kotani T., Gehrels N., 1998, ApJ, 492, 782

Yamaoka K. et al. 1999, In Preparation

Zhang S. N., Wilson C. A., Harmon B. A., Fishman G. J., Wilson R. B., Paciesas W. S., Scott M., Rubin B. C., 1994, IAU Circ., 6046

Zhang S. N., Harmon B. A., Paciesas W. S., Fishman G. J., 1995, IAU Circ., 6209